GA–A24421

TARGET FABRICATION AND CHARACTERIZATION DEVELOPMENT IN SUPPORT OF NRL LASER-PLASMA PROGRAM ANNUAL REPORT TO THE U.S. DEPARTMENT OF NAVY

JANUARY 14, 2002 THROUGH MARCH 5, 2003

by
PROJECT STAFF

Work prepared under
U.S. Department of Navy
Naval Research Laboratory
Contract No. N00173-02-C-6007

DATE PUBLISHED: AUGUST 2003

GENERAL ATOMICS

DISCLAIMER

GENERAL ATOMICS

GA–A24421

TARGET FABRICATION AND CHARACTERIZATION DEVELOPMENT IN SUPPORT OF NRL LASER-PLASMA PROGRAM ANNUAL REPORT TO THE U.S. DEPARTMENT OF NAVY

JANUARY 14, 2002 THROUGH MARCH 5, 2003

by
PROJECT STAFF

Work prepared under
U.S. Department of Navy
Naval Research Laboratory
Contract No. N00173-02-C-6007

GENERAL ATOMICS PROJECT 39083
DATE PUBLISHED: AUGUST 2003

TABLE OF CONTENTS

LIST OF FIGURES

LIST OF TABLES

EXECUTIVE SUMMARY

Key issues for the future of Inertial Fusion Energy (IFE) include the ability to manufacture large quantities of low-cost targets meeting precise specifications, and that are able to survive injection into a high-temperature IFE reaction chamber. The Naval Research Laboratory (NRL) has designed high-gain, direct-drive targets for both the IFE and the Inertial Confinement Fusion (ICF) programs. The work this year has focused on developing the scientific basis for fabricating, characterizing, and injecting high-gain, direct-drive targets.

This report describes the work conducted this year for target fabrication and characterization. A companion report documents the work done for target injection and tracking. Target fabrication research and development tasks included (1) development of high-Z overcoats for targets, (2) characterization of foam shells, (3) conducting micro-encapsulation research for target mass production, (4) experimental design of a cryogenic fluidized bed layering system, and (5) target mass production process flow and costing.

In support of these tasks, our major accomplishments included:

- Presented work and prepared publication for high atomic number target coatings, including gold and palladium.
- Characterized foam shells in index matching fluids using a newly developed optical fixture that allows viewing from two orthogonal directions without moving the shells.
- Built and tested apparatus to produce shells by the microencapsulation process, and built a prototype gas agitated contactor to test an improved method to cure the shells.
- Performed scoping studies and design calculations for an experimental cryogenic fluidized bed to be used for deuterium layering experiments.
- Prepared a process description for mass production of IFE targets with a preliminary facility layout and production cost estimates.

The target fabrication workscope this year has made significant progress in extending the knowledge base and developing a “credible pathway” for inertial fusion target fabrication. The result of these tasks is increased confidence in the overall feasibility of direct-drive inertial fusion energy.

1. INTRODUCTION

The realization of inertial fusion energy begins with the successful fabrication and characterization of high gain targets. The NRL direct-drive high-gain target consists of four parts: a DT-filled low-density foam shell with a full-density polymer "seal coat" of 1 to 5 μm, covered with a high-Z material (Au and/or Pd), a layer of solid DT fuel, and a core containing DT vapor. These targets must meet precise specifications and be mass-produced at low-cost for an inertial fusion energy plant to be feasible. These targets are filled with DT gas, lowered to cryogenic temperatures, and layered. The layering process makes use of the naturally occurring energy from beta decay of DT (sometimes supplemented by external rf or infrared energy) to heat the DT on the inner surface of the capsule. The inner temperature of the thicker portions of the layer gets warmer than the rest and ablates. This ablated DT condenses on thinner parts of the layer. Over a period of hours, this leads to a very smooth and uniform DT layer.

Target fabrication research and development tasks included (1) development of high-Z overcoats for targets, (2) characterization of foam shells, (3) conducting micro-encapsulation research for target mass production, (4) experimental design of a cryogenic fluidized bed layering system, and (5) target mass production process flow and costing. This report describes work done by General Atomics in the past year in these areas to develop the scientific basis for low-cost mass-production of the NRL direct drive target.

2. HIGH-Z COATINGS PREPARATION AND MEASUREMENT

High atomic number (Z) coatings are desirable on targets for two reasons. High Z coatings have been shown to reduce laser imprint on targets. These coatings are also highly reflective, thereby reducing radiation heating of the cryogenic targets during injection into a hot power plant reaction chamber.

Two presentations on this topic were prepared and delivered at the 2nd IAEA Technical Meeting on the Technology of Inertial Fusion Energy Targets and Chambers. They were "Thickness and Uniformity Measurements of Thin Sputtered Gold Layers on ICF Capsules" by Annette Greenwood and "Palladium and Palladium Gold Alloys as High Z Coating for IFE Targets" by Elizabeth Stephens. A paper was also written and accepted for publication: "Optimizing High Z Coatings for IFE Shells," *Fusion Science and Technology* (May 2003). These presentations and paper reported our investigations of gold and palladium for the high-Z target coatings, as summarized below.

X-ray fluorescence is used to measure high Z layer thickness on the shells. An x-ray beam is passed through the shell, which emits x-rays characteristic of the elements present. A detector captures portions of the x-rays and the resulting peaks correspond to the amount of the element present. Rotating the shells, we found that the layer thickness was uniform within the experimental uncertainty of about 10%.

Gold has a higher reflectivity than palladium. A 300 Å gold layer has an integrated reflectivity of 96% at expected power plant temperatures. The integrated reflectivity of a palladium coating at expected power plant temperatures is approximately 80%.

However, palladium is more permeable to hydrogen than is gold. High permeability is important to reduce target filling time and tritium inventories. A 300 Å gold layer reduced the rate at which deuterium permeates out of PAMS shell by a factor of 6. An 1100 Å palladium layer caused only a slight reduction in shell permeability. Layers of gold and palladium sputtered simultaneously on the shells still had very high permeability and gave reflectivity that is intermediate between the reflectivity of gold and palladium.

We performed tests to verify that the high permeation rates that were measured for hydrogen through the shells were due to catalysis rather than small cracks in the palladium or other effects. This was done by diffusing noble gases (first argon and later krypton) into the shells and performing x-ray fluorescence measurements. The measurements for argon concentration were complicated by the overlap of argon and palladium emission lines. Additionally, measurements for krypton were also inconsistent, possibly because the shells that were used for this testing had been through excessive handling. The tests with krypton will be tried again with fresh shells.

3. CHARACTERIZATION OF FOAM SHELLS

We provided characterization of divinyl benzene foam shells supplied by Diana Schroen of Schafer Corp., through her IFE work at SNL. We devised a simple means of optically characterizing these semi-opaque foam shells. This involves obtaining pictures of the magnified foam shells at two orthogonal angles using light passing through each shell that highlights the edges of the inner and outer walls.

As shown in Fig. 1, foam shells are placed in a square cuvette filled with liquid that closely matches the foam shells optical properties, allowing for distortion-free wall measurement. When we initially tried to obtain orthogonal views of the shells by rotating the cuvette 90 deg under a microscope, the shells rolled very readily assuming an orientation that was not orthogonal to the first. We solved this problem by devising a fixture that had two mirrors mounted at 22.5 deg to the vertical. Then, with the cuvette positioned between the mirrors, two views of the shells 45 deg to the vertical can be obtained. Thus the views from the two mirrors are orthogonal to each other and can be pictured without disturbing the position of the shells in the cuvette. Light is admitted through slots in the sides of the holder and reflected from a frosted, angled surface in the base. We performed a solvent exchange from water to dibutyl pthalate so the index of refraction mismatch would not distort the measurement and so it would be easier to see through the shells.

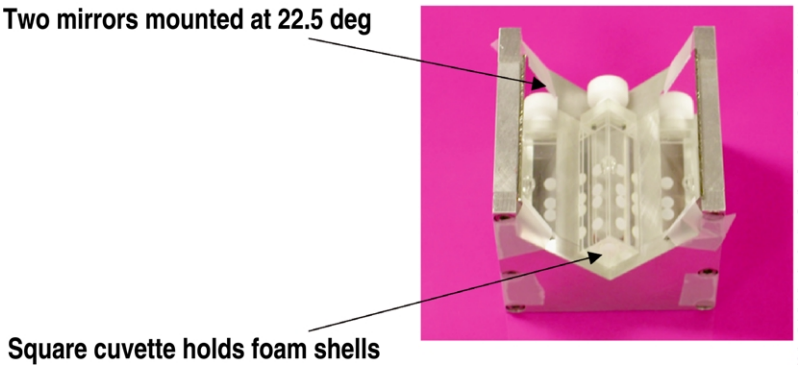

Fig. 1. The cuvette holder allowed foam shells to be viewed from orthogonal angles without rotating the cuvette and disturbing the shell position.

The positions of several points along inner and outer walls are used to calculate the “best fit” circles representing the walls. The difference between the radius of the inner circle and the radius of the outer circle is the average wall thickness. The distance between the centers of the circles is equal to the planar offset. A second picture from an orthogonal angle is used to generate additional wall thickness and offset values that are combined with the first set to

generate the average outer diameter, average wall thickness, and three-dimensional offset values.

We characterized eleven batches of foam shells. Table 1 shows a typical set of summary data we measured on the shells. Data included minimum, maximum, and average wall thickness, nonconcentricity, average inner diameter and outer diameter and out-of-round dimensions in each of the two orthogonal views.

Table 1
A Typical Set of Foam Shell Measurement Data Provided by GA[(a)]

Shell Number	Average Wall	NC Offset/Wall (%)	Wall Minimum	Wall Maximum	Δ Wall Max – Min	Average o.d.	Average i.d.
1J5 114A #1	230	31	158	301	143	3952	3492
1J5 114A #2	246	23	188	303	115	3934	3442
1J5 114A #3	238	41	140	336	196	3964	3488
1J5 114A #4	244	29	172	316	144	3982	3493
1J5 115A #1	251	34	165	336	171	3991	3490
1J5 115A #2	250	17	207	292	85	4025	3526
1J5 115A #3	244	9	221	267	45	4026	3538
1J5 115A #4	250	13	217	282	66	4037	3538
1J5 116A #1	247	16	208	285	76	4017	3524
1J5 116A #2	248	11	221	275	54	4039	3543
1J5 116A #3	252	18	205	298	93	4026	3523
1J5 116A #4	246	7	230	263	33	4028	3536
1J5 117A #1	250	20	200	301	101	4061	3560
1J5 117A #2	266	42	155	377	221	4069	3537
1J5 117A #3	249	13	218	281	64	4072	3574
1J5 117A #4	246	17	205	287	83	4077	3585

[(a)]Units of shell dimensions are microns. NC is percent nonconcentricity, defined as offset divided by wall thickness.

One of the main problems identified by our foam shell characterization is nonconcentricity. Nonconcentricity is the maximum distance between the center of the shell inner wall and the center of the shell outer wall divided by the average wall thickness. Schafer is working with density matching, temperature control and agitation to improve concentricity.

The shells are quite fragile and are easily cracked when handled. Figure 2 illustrates an example of a cracked shell. About 25% of the shells were cracked after shipping to GA and nearly 95% were cracked after the solvent exchange process. To minimize the amount of shell damage, it was ultimately decided to begin characterizing the shells onsite at SNL.

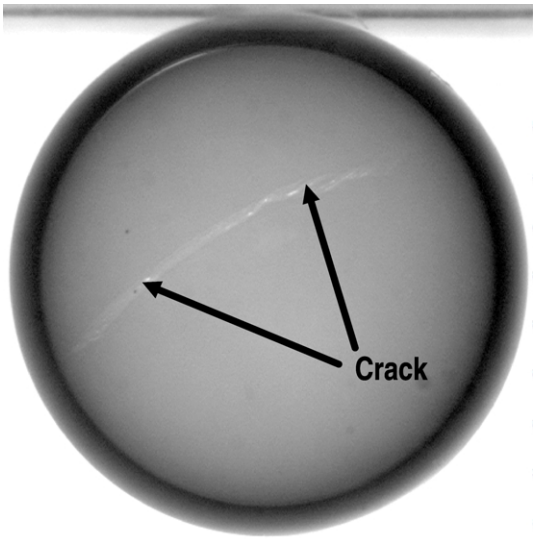

Fig. 2. Foam shell with crack that may have been induced from handling.

4. MASS PRODUCTION LAYERING

Demonstration of mass-production layering is a high priority for target fabrication. Our studies for mass production layering were reported at the April 2003 HAPL meeting. The presentation viewgraphs are included in the Appendix and are summarized here.

Mass production layering processes must be quite different than the layering sphere process that is currently used for direct-drive single target layering. One possibility is the fall and strike technique that the Russians are investigating at Lebedev Physical Institute. We support the fall and strike study as a potential backup,[1] and will learn what we can from this study, but we do not believe that we can rely on fall and strike as the only layering method. We are focusing our efforts on the fluidized bed approach.

Relatively simple equations have been used to estimate the time required for a target to circulate through a fluidized bed. The circulation time depends on the gas velocity, density, viscosity, density and the particle density and diameter, and the height of particles in the fluidized bed. A typical example is given for a fluidized bed with a circulation time of 0.27 s; the temperature difference from top to bottom of the bed is only 0.054 K. This rapid circulation and small temperature gradient is calculated to lead to only 3 mK temperature changes at the inner surface of the DT ice in one circulation time.

In a target factory, the capsules would be loaded into a cell and permeation filled at room temperature with DT. The capsules would then be cooled and dropped into a fluidized bed. The targets would be further cooled in the bed by a closed loop helium flow. The helium compressor would be inside the cryogenic environment to minimize the cooling power requirements. The gas flow for a fluidized bed with full sized targets is quite large, 1.8 g/s, and has large cooling requirements. We are evaluating the trade-offs with a scaled-down fluidized bed demonstration experiment.

[1]Letter of support was sent on January 13, 2003 to ISTC supporting the proposed 5-year study at Lebedev Physical Institute entitled “Development of a facility for producing the reactor-scaled cryogenic targets and their repeatable assembly with sabots.”

5. MICROENCAPSULATION RESEARCH

We performed research and development to examine scaleup opportunities, utilizing chemical engineering principals and apparatus, to understand the science behind mass production of IFE targets. Specifically, we focused our efforts on producing 4.6 mm/250 μm wall polystyrene direct drive targets to produce a stock of targets for additional coating and layering studies, and designed and tested apparatus for mass production of direct drive targets. This information can be applied to the formation of indirect drive targets in future studies as well because many of the processes and apparatus are similar.

A presentation on this topic was prepared and delivered at the 2nd US/Japan Workshop on Target Fabrication, Injection, and Tracking, February 3–4, 2003, "Microencapsulation Studies for Mass Production of IFE Targets" by Brian Vermillion. This presentation reported our investigation into understanding the science of producing IFE targets as summarized below.

The microencapsulation process involves producing multiphase drops or shells in a triple orifice droplet generator. As illustrated in Fig. 3 for making poly-α-methylstyrene (PAMS), targets, an inner drop of water (aqueous phase) is surrounded by a mixture of PAMS dissolved in fluorobenzene (nonaqueous polymer solution).

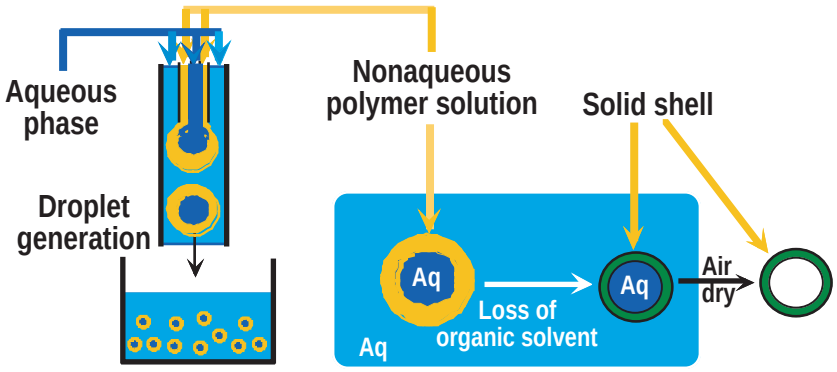

Fig. 3. Schematic of PAMS microencapsulation.

The drop forms by flowing the two solutions through a triple orifice generator (Fig. 4). A stripping flow of polyacrylic acid (PAA) in aqueous solution then strips the drop from the orifice needle at a predetermined rate for a particular size drop (outer aqueous phase). Flowrates vary depending upon the diameter and wall thickness of drop desired. For example, typical flowrates for 2 mm diameter shells with 20 μm walls are 40 cc/h of inner water and 14 cc/h of the polymer solution, with the outer flow varied to strip the drops at about one per second, usually 3600 cc/h.

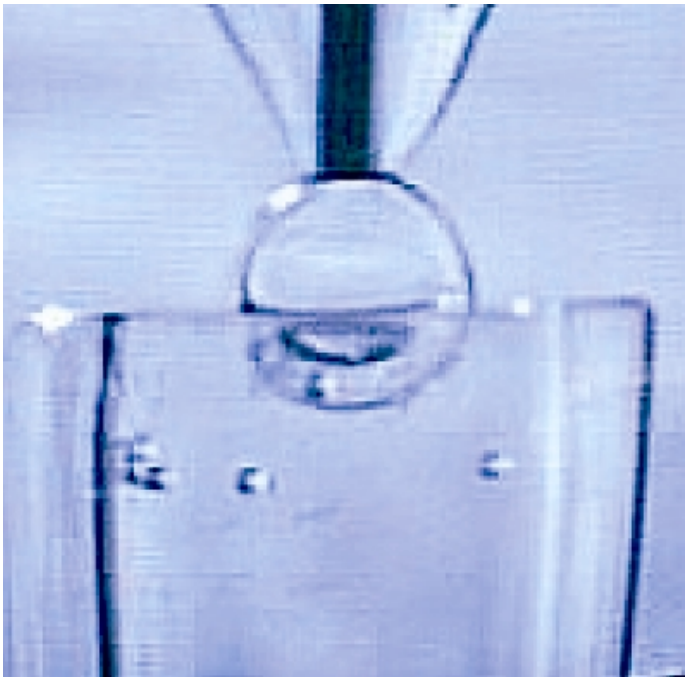

Fig. 4. Droplet formation.

Once the desired quantity is produced, the collected drops, or shells, are hardened by removal of the fluorobenzene solvent from the nonaqueous polymer solution in rotary evaporator containers warmed in water baths. Once the shells are solid, they undergo several washes to remove particulate contamination and debris from the shell surface. At this point, ethanol extraction of the water inside the shell is performed. The shells are then placed inside a vacuum oven at 25°C for approximately two weeks to completely dry the shells.

The triple orifice microencapsulation process is deceptively simple with few process variables to manipulate. However, small changes in these variables can cause large and sometimes unanticipated changes in final shell characteristics. For example, if it is desired to shorten the time it takes to remove fluorobenzene solvent from the hardening shells, one could increase the water bath temperature. However, this leads to significant changes in the solubility of the polymer solution in the aqueous phase increasing surface roughness, density changes in each phase leading to density mismatch, viscosity changes of the solutions affecting agitation during hardening, and interfacial surface tension changes affecting shell concentricity. Thus, one process variable change (water bath temperature) can lead to significant alterations in final shell characteristics.

The IFE Microencapsulation Laboratory is up and operational (Fig. 5) with initial shakedown and experimental runs complete. Figure 6 shows 3 mm shells from an initial test run. In Table 2, simplified characterization results are available for review of two initial runs.

Fig. 5. Microencapsulation laboratory.

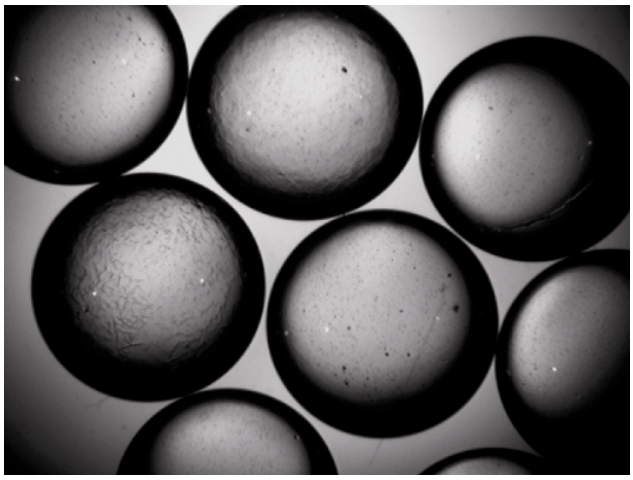

Fig. 6. 3 mm diameter/30 μm wall polystyrene targets made in ME laboratory.

Table 2
Characterization of Initial Runs

Specifications[(a)]	Run 3	Run 4
Estimated diameter	2300 μm	3003 μm
Diameter ±5%	2387 μm	3013 μm
Estimated wall thickness	24 μm	30 μm
Wall thickness ±10%	23 μm	32 μm
OOR, <1.0% of radius	0.44%	0.36%
NC, <1% to 5%	NA	1.4

[(a)]For these runs only.

Mass production of IFE targets differs from the aforementioned lab scale process in significant ways, as our goal is to form at least 500,000 targets per day in what will most likely be a continuous process. All aspects and assumptions of the process require review to identify which areas need to be altered. The first such arena to explore are the liquid ratios used in the laboratory scale process. Defined as volume of solution plus targets per the volume of targets, the lab scale ratio is 200 to 1, while production scale will assume a ratio of 10 to 1. Even with this lower ratio, up to 3,000 L of aqueous phase fluid will be required per 100,000 unit run. Therefore, we have identified the need for a recycle stream to be implemented in the droplet generation process, including a way to remove contaminants from the recycle stream.

Additionally, a parametric study needs to be undertaken to determine the flowrates required for larger IFE targets. While larger diameter targets have been successfully formed in the past (5 mm), they were formed with a thin wall, ~1% of diameter. The flow parameters for thicker walled targets can be theoretically determined, but will have to be confirmed in the laboratory since a different flow regime than is currently used will be required. Specifically, the ratio of the inner aqueous flow to nonaqueous polymer flow is generally 2.8 to 1 for smaller targets (3 mm targets), but will have to altered to 1 to 2.3 for larger 4.6 mm/250 μm wall targets. The effect this will have within the droplet generator needs to be determined and will require a redesign and modification to the apparatus itself for larger diameter targets.

Another aspect to explore is the optimization of the cure times for solvent removal from the nonaqueous polymer solution. Unfortunately, one cannot simply increase the rate of solvent removal, as is explained below. Surface defects are believed controlled by the Marangoni Effect [1], represented by the equation:

$$M = \frac{\left(\frac{d\gamma}{dc}\right) \times \Delta C \times L}{\eta \times D} \quad ,$$

where $(d\gamma/dc)$ is the change of surface tension with concentration, ΔC is the concentration gradient perpendicular to the surface, L is wall thickness, η is the polymer viscosity, and D is the diffusivity of fluorobenzene within the polymer solution. If the Marangoni number is too large, concentration cells form in the wall of the shell, leading to uneven surfaces on the targets. In order to control these defects, we have in the past decreased both the surface tension and concentration gradient to lower the Marangoni number. However, in the case of targets with thicker walls (L = 250 μm), we are once again increasing the Marangoni number. But if we simply reduce the same parameters, surface tension and concentration gradient, then curing time is greatly extended.

Additional scaleup opportunities have been identified for mass production. Currently, rotary contactors, Fig. 7, are used to remove solvent from and cure the targets. However, the contactors are not easily scaled to different and larger sizes and will require parametric studies to determine what process parameters, such as rotation speed and internal configuration, will not damage the targets.

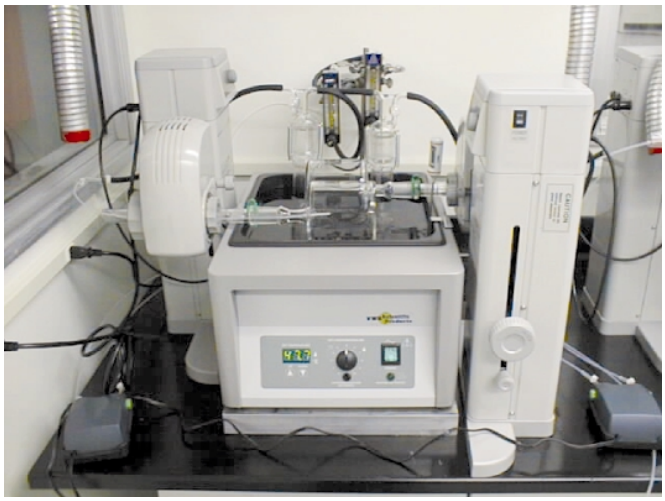

Fig. 7. Rotary contactors for removal of solvent.

To address the problem of scalability, we have developed a prototype gas agitated contactor, GAC, pictured in Figs. 8 and 9. The apparatus uses a three-phase contact of solvent (fluorobenzene) saturated air, outer aqueous bulk fluid, and the semi-solid targets to remove solvent in a controlled, optimized manner.

Fig. 8. Prototype GAC.

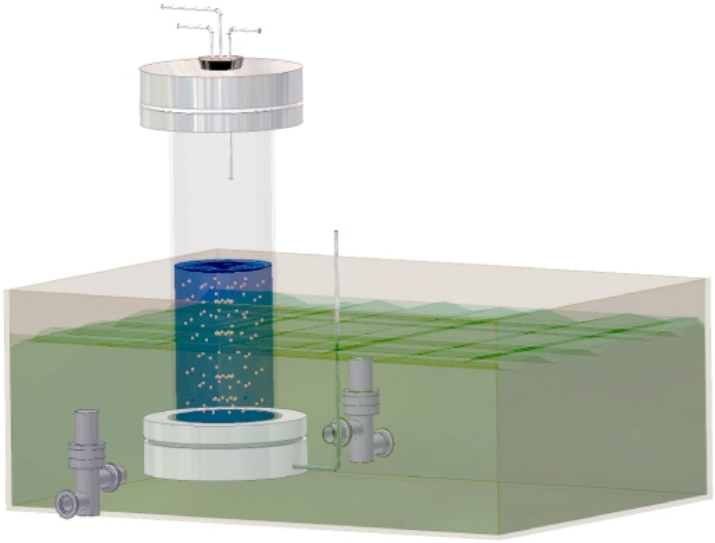

Fig. 9. Schematic of GAC.

The GAC could possibly replace the rotary contactors in future mass production scenarios. The design is eminently scaleable in the x-y direction once away from wall effects, without having to identify new process parameters by repeating time consuming parametric studies. An added benefit is that the design is easily adaptable to a continuous process, ideal for a large facility in the future. Functional attributes include using a controlled mixture of air and fluorobenzene bubbles to remove fluorobenzene from the system and gently agitate the shells as pictured in Fig. 10. This apparatus can also be used for subsequent washings and water/ethanol extractions without exposing the targets to contamination or the stress of being moved from container to container as is currently done. The design and fabrication is complete with test runs under way as pictured in Fig. 10.

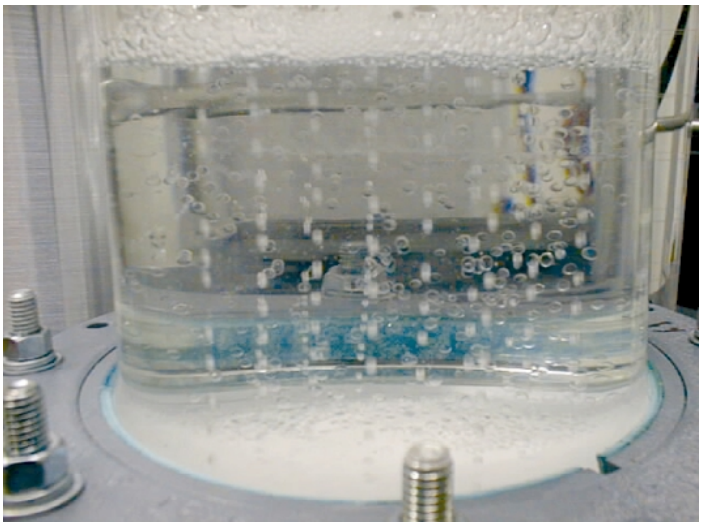

Fig. 10. GAC in use.

The GAC will require foam minimization in order to be fully functional. We have identified that while the 0.05 wt% PAA aqueous stripping solution does not foam, the 0.3 wt% to 3.0 wt% polyvinyl alcohol (PVA) aqueous solutions used to clean debris off the shells do foam. Therefore, a new washing solution with dual roles will have to be identified with the ability to wash PAA off targets without foaming and that can be utilized in a continuous process without excessive cost. Several solutions have been identified for testing: DI water, isopropanol, ethylene glycol, sodium hydroxide, and acetic acid.

Another area identified for process improvement is the droplet generator apparatus currently used for making the targets. A handmade glass needle is employed in the system. Several shapes of this needle are in use in different generators with each one requiring different flowrates to achieve a shell with similar characteristics. This is not conducive to mass production, as it would be expensive and time-consuming to identify and reestablish flowrates every time a fragile glass needle requires replacement. Therefore, we have begun a redesign of this particular element of the droplet generator via a metal needle replacement. This needle will be self-centering as well as made of metal in order to have a consistent design to refer back to in case the part needs to be replaced. It is anticipated that designs with slight variations will need to be tested to ensure adequate operation, but once identified, will provide a vast improvement in repeatability and consistency.

Near term work goals for microencapsulation research and development include the following: identify and confirm experimentally the required flowrates for larger diameter targets, examine alternative washing solutions for use in the GAC, and optimization of solvent removal rates within the new GAC apparatus. Additionally, longer-term research will focus on adding process control to the microencapsulation process in order to better control and increase the yield of acceptable targets. This will most likely entail optical imaging systems to examine targets that have not yet been cured in real time, adding a pulse system to control target formation to speed up generation and reduce debris in the stream, as well as exploring forced convection while the shells are drying. A current idea is to include forced convection with dry nitrogen, cycled with applications of vacuum, to draw out the remaining ethanol from within the target interior.

6. MASS PRODUCTION TARGET FABRICATION PROCESS FLOW AND COSTING

The "Target Fabrication Facility" (TFF) of a 1000 MW(e) IFE power plant must supply about 500,000 targets per day. The feasibility of developing successful fabrication and injection methodologies at the low cost required for energy production (about \$0.25–0.30/target, about 10^4 less than current costs) is a critical issue for inertial fusion.

To help identify major cost factors and technology development needs, we have utilized a classical chemical engineering approach to the TFF. We have identified potential manufacturing and handling processes for each step of production and have evaluated the raw materials, labor force, cost of capital investment, and waste handling costs for providing 500,000 direct-drive targets per day. We have prepared preliminary equipment layouts and determined floor space and facility requirements. This work was presented at the 2nd IAEA Technical Meeting on the Technology of Inertial Fusion Energy Targets and Chambers, has been published in *Fusion Technology* [2], and is summarized here. A detailed technical report has also been prepared [General Atomics Report GA–C24190 provided to the primary customer (NRL)] which would allow a full peer review of the calculational approach and all of the assumptions that have been used in estimating the capital and operating costs.

This modeling methodology is intended to provide a first cut at the facility design concepts and cost, a framework to compare and contrast future design decisions, and a tool to help guide future research directions.

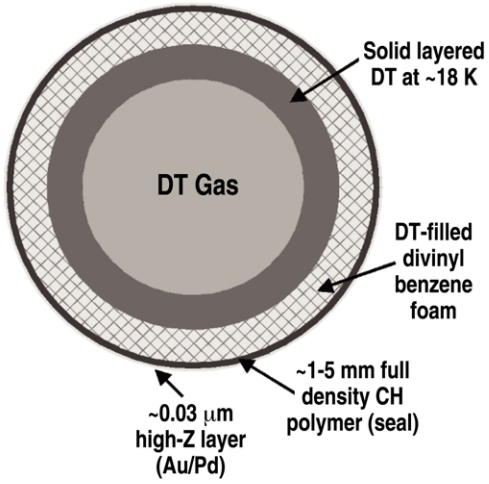

Fig. 11. Finished NRL direct-drive high-gain cryogenic target.

6.1. PROCESS DESCRIPTION

Following are descriptions of each of the 13 major process steps leading to a filled, layered target (as shown in Fig. 11) that is ready for injection [3]:

Process Step #1 — Divinylbenzene (DVB) foam shells are made with a dibutyl phthalate foam solvent and a 2, azo-bis-iso-butyronitrile (AIBN) initiator (for subsequent DVB cross-linking). Water is inside the hollow targets and water/PVA is on the outside. These targets flow with the outer water into rotary contactors where the targets comprise ~8% of the contactor total volume (a lower solids ratio may be used for the initial process stage where the targets are not yet fully cured and are thus more fragile).

Process Step #2 — The freshly formed DVB targets are gently stirred by the rotation of the contactor as the foam partially cross-links at ambient temperatures.

Process Step #3 — The partially cross-linked targets are heated to 85°C to more fully polymerize and cross-link the DVB foam.

Process Step #4 — Isopropanol is sufficiently miscible in both water and oil (parachlorotoluene) to facilitate the transition from inner water (step #1–3) to inner oil (step #5).

Process Step #5 — Oil (parachlorotoluene) is transferred into the targets to provide a medium for Monomer A (isophthaloyl dichloride) to subsequently be dissolved into (in step #6).

Process Step #6 — Monomer A is dissolved into the oil inside of the targets.

Process Step #7 — Water/surfactant replaces the oil outside of the targets, keeps them from sticking together, and provides an aqueous medium for Monomer B (poly 4-vinyl phenol) to be dissolved in Step #8.

Process Step #8 — Monomer B is added to the water/surfactant to initiate the formation of the 1–5 μm thick seal coat via polymerization of Monomers A and B at the oil/water interface on the target surface.

Process Step #9 — Isopropanol is sufficiently miscible in both oil (parachlorotoluene) and CO_2 to facilitate the transition from inner oil/outer water (step #8) to inner/outer CO_2 (step #10).

Process Step #10 — Liquid subcritical CO_2 (20°C–800 psig) replaces the inner IPA by countercurrent stagewise dilution contacting. The resulting liquid-CO_2 filled targets are heated beyond the CO_2 critical point (31°C–1070 psig) to reduce surface tension to zero and thus prevent target stress fracturing from depressurization forces during subsequent venting of the supercritical CO_2. This results in dry targets with only ambient pressure gaseous CO_2 inside/outside, ready for the high-Z coating in step #11.

Process Step #11 — A thin (~0.03 μm) gold and/or palladium coating is added to the outer surface of the dried targets by a batch sputtering process (i.e., physical vapor deposition) performed in a vacuum (which removes the gaseous CO_2 remaining in the target from step #10).

Process Step #12 — DT is loaded into the targets by diffusion at high pressures (at room temperature or above) followed by condensation at cryogenic temperatures (≤20 K) to lower the internal pressure in the targets to prevent target rupturing as the external pressure is reduced.

Process Step #13 — DT-filled targets are maintained at a temperature slightly below the triple point while they are gently fluidized with gaseous helium (to maintain a time-averaged

highly isothermal temperature profile on the entire surface of the sphere) and exposed to a heating beam that will result in preferential sublimation at thicker areas and eventually yield a uniform DT layer.

6.2. PROCESS FLOW AND FACILITY LAYOUT

The plant conceptual design includes a process flow diagram, mass and energy balances, equipment sizing and sketches, storage tanks and facility views (plan, elevation and perspective).

The preliminary plant layout is illustrated in Fig. 12. The TFF will operate on a batch-continuous mode wherein batches of targets are placed in rotary contactors (see Fig. 13) for a series of chemical processes to yield resultant wet, overcoated shells (through step 9). After the wet targets are removed from the rotary contactor, they are then dried, sputter coated and DT-filled in batches prior to being layered in a continuous delivery to the target injection system.

6.3. CALCULATIONAL APPROACH

A detailed material and energy balance (M&EB) was prepared to provide information on the flow rates and quantities of raw materials, finished products and by-products for the entire TFF. All of the cost calculations for chemicals, utilities and waste disposal use mass quantities calculated in the M&EB.

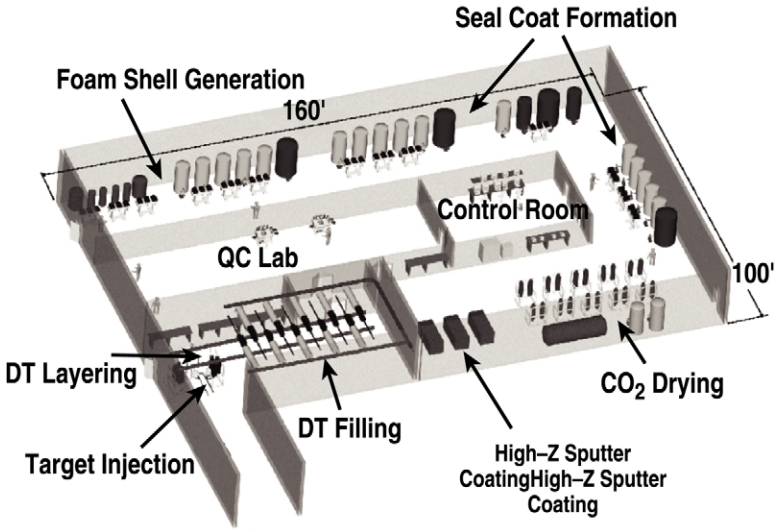

Fig. 12. IFE target fabrication facility isometric view; entire facility is about 16,000 square feet floor space.

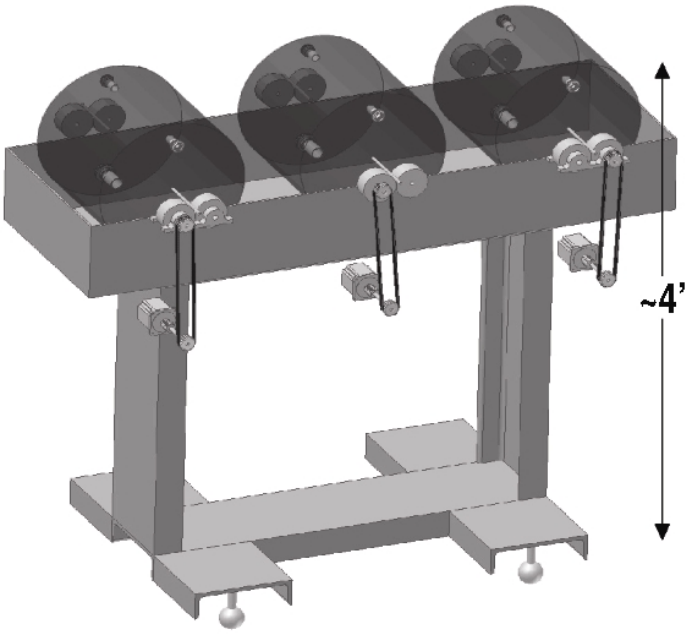

Fig. 13. Rotary contactor — a basic functional unit of the TFF.

Statistical sampling of target batches will be performed at every process step to avoid unnecessary further processing of off-spec targets. Finished dried shells with high-Z coatings will be sampled (100% QA in a final "flow-through" step) and stockpiled (potentially at a central facility serving multiple power plants) to assure a reliable supply backlog of several days of on-spec empty targets. The empty targets need only then be DT-filled and cryo-layered prior to injection. Overall target QA rejection rates are arbitrarily assumed in this work to be 25% with sensitivity studies covering a wider range of 5% to 75% reject rates. (The 25% reject rate is only a conservative assumption for calculational purposes; reject rates for a mature plant are expected to be much less than 25%.)

6.4. COST ESTIMATION

The cost estimate includes both capital and operating costs. Capital costs are broken down into purchased equipment, engineering/contingency, buildings/auxiliaries and piping/electrical/instrumentation. Operating costs are broken down into operating staff, chemicals, maintenance, utilities and waste disposal. Sampling and inspection equipment and staffing costs are included at all stages of target preparation. Where appropriate, initial discussions are underway with vendors of commercial equipment that may be used in the facility. In other cases, the costs of new or novel equipment have been estimated using engineering judgment followed by peer feedback from researchers skilled in these areas of expertise.

A generous operating staff has been allocated to the operations. There are 12 staff working a normal "5/8 day shift"[2] and an additional 28 production personnel present per shift to operate the facility. The model assumes 5-shift operation to cover 24/7 operations along with vacations, holidays, etc. Job categories include operators, technicians, health physicists, QA/QC specialists, supervisors, engineers and clerks.

Maintenance expenses are calculated using a factored percentage (6% per year) of installed capital costs. Utilities, waste disposal and chemical costs were calculated using vendor-supplied prices coupled with M&EB mass flow requirements.

6.5. MODEL SENSITIVITY RESULTS

Results of the base-case model are shown in Fig. 14, including itemized summaries of capital and operating costs on a per injected target basis. For the baseline design assumptions, the cost per target is 16.6¢. We also looked at the sensitivity of this result to changes in one or more of the assumptions. The results are given in Table 3. These single and multiple variable responses illustrate that the costs per injected target are within a 25¢ cost goal even with significant increases in assumptions.

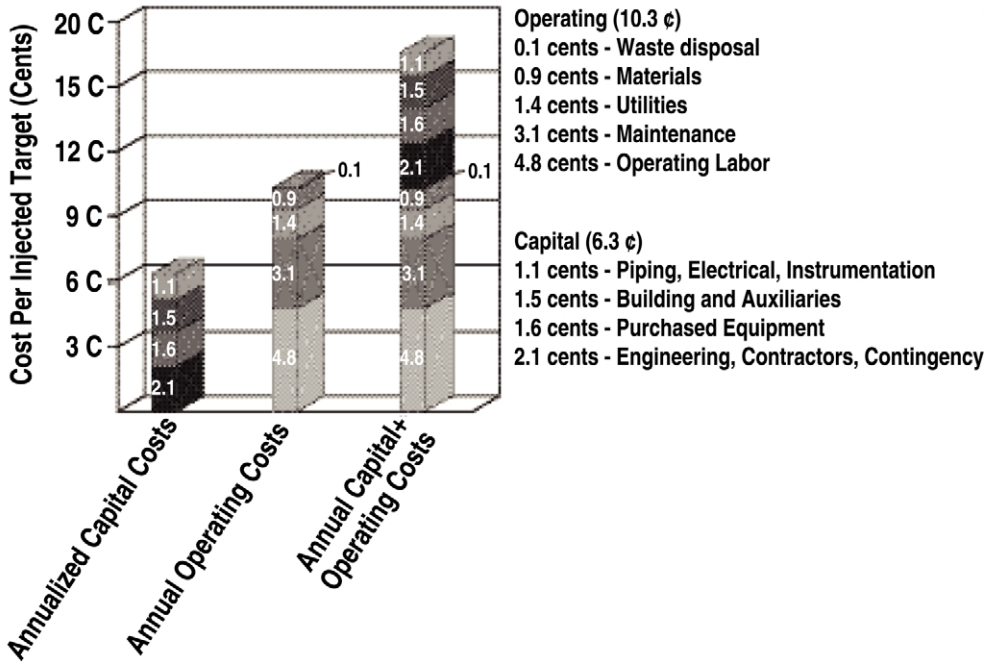

Fig. 14. Projected capital and operating costs per injected target at a 1000 MW(e) power plant.

[2] A 5/8 day shift is nominally 5 days per week less vacation and holidays.

Table 3
Results of Model Sensitivity Studies

Case	Description	Cost per Injected Target (¢)
Single variable responses [1000 MW(e) plant]:		
1	Baseline (@25% reject rate)	16.6
2	Doubled staffing costs	21.3
3	Doubled capital costs	25.3
4	Doubled maintenance costs	19.6
5	Doubled utilities costs	18.0
6	Baseline (@5% reject rate)	15.6
7	Baseline (@50% reject rate)	18.7
8	Baseline (@75% reject rate)	24.4
Multiple variable responses [1000 MW(e) plant]:		
9	All costs 25% higher and 50% reject rate	24.0
Larger plant case:		
10	3000 MW(e)	10.0

Significantly lower costs on the order of ~10¢ per injected target are calculated for a 3000 MW(e) plant. Additional cost savings of 10%–15% are possible by fabricating the empty dried targets at a central facility and then filling/layering/injecting them at the power plant site. The empty, dried shells are estimated to cost only 2.8¢ per target when made in this large quantity [10,000 MW(e) equivalent]. This economy of scale results in a savings of 0.8¢ per injected target (or 8% cost reduction) at a 3000 MW(e) plant and a savings of 2.1¢ per injected target (or 13% cost reduction) at a 1000 MW(e) plant.

6.6. PROCESS DEVELOPMENT PLAN

To achieve the cost projections discussed above, a significant technology and process development program will be required. A three-phase program is envisioned to develop process unit operations for the production of layered, D_2-filled targets — starting at lab-scale and ending at a commercial prototype. The objective of Phase 1 is to develop laboratory-scale methods and apparatus for the production of layered, D_2-filled targets. The objective of the second phase is to develop an integrated set of full-scale process unit operations. The objective of the third phase is to parametrically test equipment in sequential campaigns to produce finished DT-filled targets, and to modify equipment to attain product specifications and throughput/reliability goals. The resultant facility is ready for use as a commercial prototype.

6.7. CONCLUSIONS

A facility flowsheet, plant layout and cost model have been formulated using classical chemical engineering principles to scaleup current laboratory fabrication methods.

The cost of injected targets is estimated to be ~17¢ each for a 1000 MW(e) power plant. For the baseline assumptions, the annualized capital costs represent roughly 40% of the cost per target while annual operating costs are ~60% [for large power plants in the 1000–3000 MW(e) range]. Economies of scale (in terms of capital equipment, staffing and overhead) favor larger plants. Capital and operating costs both increase less rapidly than production rate increases, which leads to lower unit costs [from 16.6¢ per injected target at 1000 MW(e) to 10.0¢ per injected target at 3000 MW(e)].

These projections assume that a significant process R&D program (summarized herein) is successfully completed.

7. SUMMARY

Target fabrication work at GA is focused on five major areas that are briefly summarized in the following paragraphs.

We prepared presentations and publications for our study of high Z coatings on IFE targets. Gold has higher reflectivity (which is beneficial to reduce in-chamber target heating) than palladium. However, palladium has higher permeability to hydrogen to allow more rapid target filling and reduced tritium inventories in the target fabrication plant. A combination of the two metals may be an optimum coating.

We characterized foam shells produced by Schafer Inc. We used index matching fluid and a new fixture that we developed to observe the targets from two orthogonal directions. Measurement data were provided for minimum, maximum, and average wall thickness, nonconcentricity, average inner diameter, outer diameter, and out-of-round dimensions. Methods to improve the identified nonconcentricity are being worked on by Schafer.

We performed scoping studies and calculations for a cryogenic fluidized bed target layering system. Based on this work, a fluidized bed layering experiment is being designed to demonstrate deuterium layering using this method.

We produced 3-mm diameter polystyrene shells using a triple orifice micro-encapsulation technique. A gas agitated contactor was designed and implemented to potentially improve shell curing time and quality. Several scaleup opportunities were identified and preliminary work begun.

We proposed a process and facilities for mass producing direct drive IFE targets. A baseline cost estimate of 16.6 cents per injected target was obtained in this study.

ACKNOWLEDGMENTS

This report was prepared for the U.S. Department of Navy, Naval Research Laboratory Contract No. N00173-02-C-6007.

REFERENCES

[1] B.W. McQuillan, M. Takagi, "Removal of Mode 10 Surface Ripples in ICF PAMS Shells," Proc. 14th Target Fabrication Specialists Meeting, West Point, New York, 2001, to be published in Fusion Technology; General Atomics Report GA–A23747 (2002).

[2] W.S. Rickman, D.T. Goodin, "Cost Modeling for Fabrication of Direct Drive IFE Targets," Fusion Science and Technology (May 2003).

[3] J. Streit, D. Schroen, "Development of Divinylbenzene Foam Shells for Use as Inertial Fusion Energy Reactor Targets," Fusion Science and Technology (May 2003).

APPENDIX
MASS PRODUCTION LAYERING FOR IFE

Mass Production Layering for Inertial Fusion Energy

presented by
Neil Alexander

HAPL Project Review
Albuquerque, New Mexico
April 9, 2003

Los Alamos
NATIONAL LABORATORY

Topics

- Introduction - target supply
- Concepts for mass-production layering
- Design calculations for a cryogenic fluidized bed demonstration
  - transit/residence time
  - cooling requirements
  - experimental designs
- Conclusions - and some choices to make (inputs solicited!)

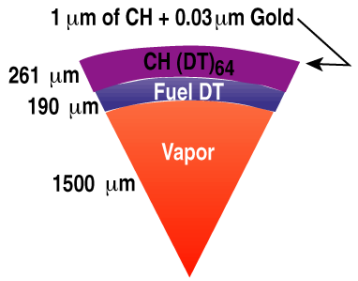

NRL High Gain Direct Drive Target

Cryogenic fluidized bed has been proposed

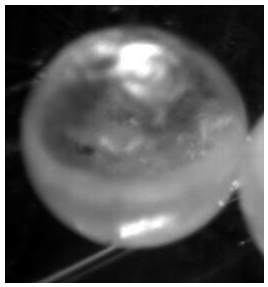

Before

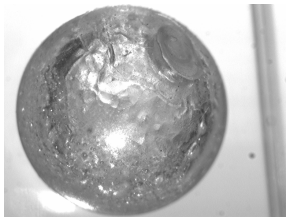

After

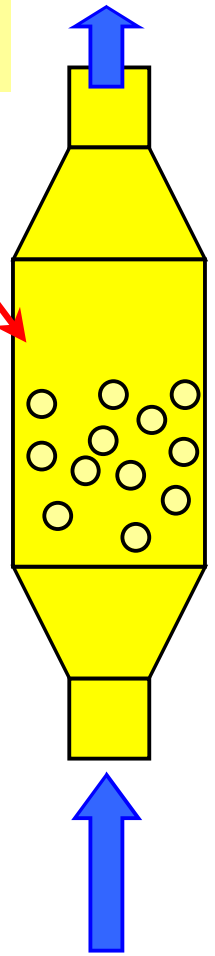

Neopentyl alcohol as surrogate for hydrogen - proof of principle demo

Los Alamos NATIONAL LABORATORY

Mass-production layering methodology is unique to IFE

- Objective = support IRE/ETF with a "credible pathway" position for every aspect of the IFE target supply process
- Most target supply steps have a clear prior experience base (e.g., ICF program)
  - capsule fabrication (microencapsulation)
  - high-Z overcoating (sputter coating)
  - characterization (optical, others)
  - filling of capsules (permeation filling)
- Cryogenic layering has a demonstrated principle (beta-layering), but the methodology is different for IFE
  - NIF is using in-hohlraum layering
  - LLE is using individual layering spheres
- IFE must provide a reasonable path for layering large numbers of filled capsules
  - the major remaining issue for target fabrication in the near-term

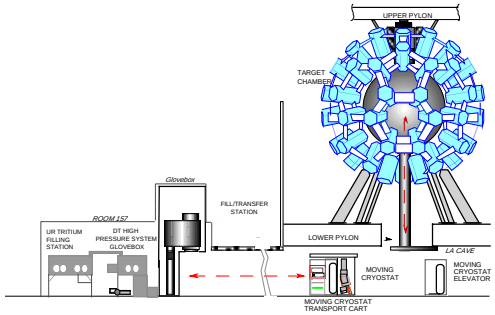

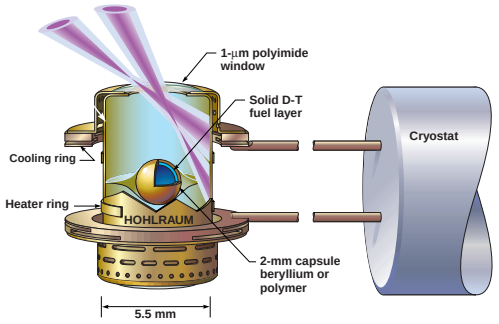

.... method will likely involve mechanical motion and slow freezing

Los Alamos NATIONAL LABORATORY

We support the Russian proposal for a Fall & Strike" layering demo

- Elena Koresheva has proposed a FST layering demo with handoff to an injector
  - proposed five year program at Lebedev/Moscow
  - funding would come from International Science and Technology Center (ISTC)
- We support this work as potential backup, but believe that HAPL cannot rely on it
- We will follow the ISTC program and learn as much as we can from it (we are an "official collaborator", letter of support sent to ISTC)

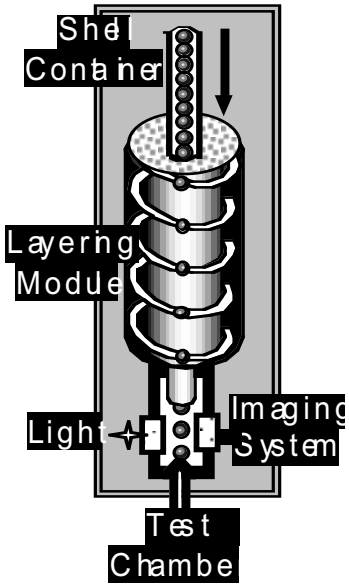

Fig. 1. Layering module with a spiral channel.

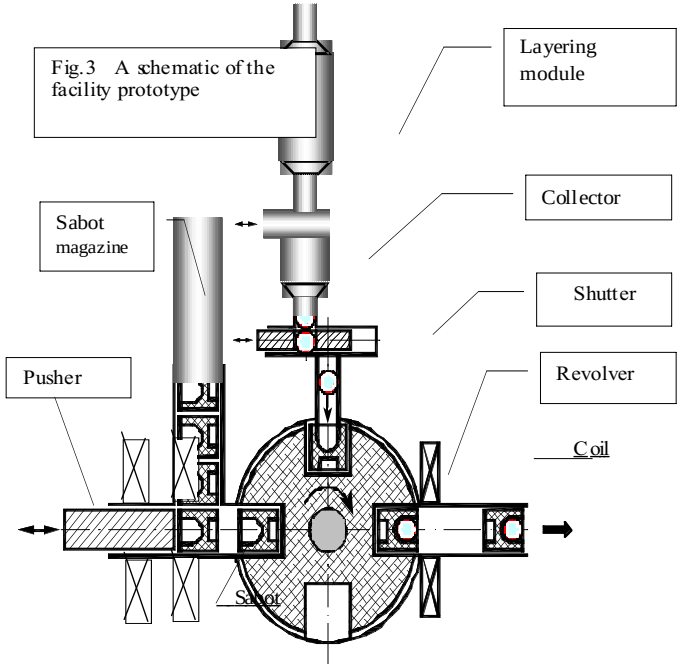

Los Alamos NATIONAL LABORATORY

The circulation time of a target in the bed can be estimated

The circulation time of a particle in a fluidized bed is given by Rowe as

$$t_p = \frac{H_{mf}}{0.6\left(U - U_{mf}\right)\left[1 - \left(\frac{U - U_{mf}}{U_b}\right)\right]}$$

Where
H_{mf} is the height at minimum fluidization (~settled height),
U is the superficial velocity of the gas,
U_{mf} is the minimum velocity for fluidization,
U_b is the bubble (gas in particles) velocity.

Yates combines the Ergun equation with the empirical results of Wen and Yu for minimum fluidization voidage to obtain

$$U_{mf} = \frac{\mu}{d_p \rho_g}\left(\left\{33.7^2 + 0.0408\frac{d_p \rho_g\left(\rho_p - \rho_g\right)g}{\mu^2}\right\}^{1/2} - 33.7\right)$$

Where
μ is the viscosity,
d_p is the particle diameter,
ρ_g is the density of the gas,
ρ_p is the density of the particle,
g is the acceleration of gravity.

Inputs required provided from bed design
— except bubble velocity, U_b

Los Alamos
NATIONAL LABORATORY

Expressions exist for bubble velocity

Davidson and Harrison give the average bubble velocity as

$$\overline{U}_b = \left(U - U_{mf}\right) + 0.711\left(g d_b\right)^{1/2}$$

Where
d_b is the bubble diameter.

Yates gives that bubble diameter as

$$d_b = \frac{0.54\left(U - U_{mf}\right)^{2/5}\left(h + 4\sqrt{A_0}\right)^{4/5}}{g^{1/5}}$$

Where
h is the height of the bubble in the bed,
A_0 is area of the distributor per orifice in the distributor (=0 for a porous plate; we assume this).

Note: main free parameter is height of bed
— also gas density, but this can not be too high or targets will be crushed
- – gas type limited by temperatures to helium and possibly hydrogen

An example circulation time

The circulation time of a target in the bed can be short

Using helium gas at 380 torr to leviate that bed with

d_p = 3.956 mm,

particle (target) mass = 0.004 gm,

H_{mf} = 4.4 cm

χ = 2 (fluidized bed height of $2*H_{mf}$=8.8cm),

properties evaluated at 18 K,

U = 132 cm/sec (from design section type calculations), and

U_{mf} =36 cm/sec.

$d_b = 1* d_p$, $7* d_p$, and $12* d_p$, for h = d_p, H_{mf}, and $2*H_{mf}$ respectively.

Utilizing $d_b = 7*d_p$ gives

t_p = 0.27 sec.

NOTE: The temperature difference (ΔT) of this bed top to bottom is 0.054 K.

Eight (8) beds with diameter 32 cm and this height can supply targets at a 6 Hz rate
– assuming 8 hrs to fill and cool, 13 hours to layer, and 3 hours to unload

Los Alamos
NATIONAL LABORATORY

Short circulation times mitigate effect of ΔT at inner ice surface

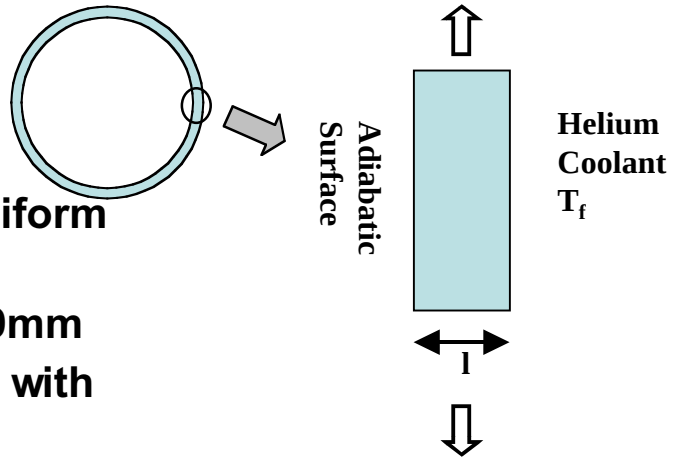

Approximate target as infinite slab with finite width

Transient thermal solutions are available for an initially uniform temperature slab (see Figure 4-6 in Eckert and Drake)

The above conditions with slab thickness l=0.479mm produce the following dimensionless parameters to utilize with solution plots

x/l = 0 (ie inner surface),

$$\frac{k}{hl} = 4$$

$$\frac{\alpha\tau}{l^2} = 0.4$$

Where
k is DT thermal conductivity(0.30 watt/(m*K))
h is the helium film heat transfer coefficient(167 watt/(m^{2}K),
α is DT thermal diffusivity (3.4x10^{-7} m^2/sec),
l is DT thickness,
t is time (set to t_p= 0.27 sec).

Solution plots yield that an initial 0.054K coolant (helium) perturbation produces only (1-0.95)*0.054K=0.0027K temperature change at the inner ice surface in one circulation time.

Thus, the inner ice will experience very small temperature changes.

Los Alamos NATIONAL LABORATORY

GENERAL ATOMICS
AND AFFILIATED COMPANIES

Target factory implementation

Capsules are loaded into cell and permeation filled at room temperature with DT

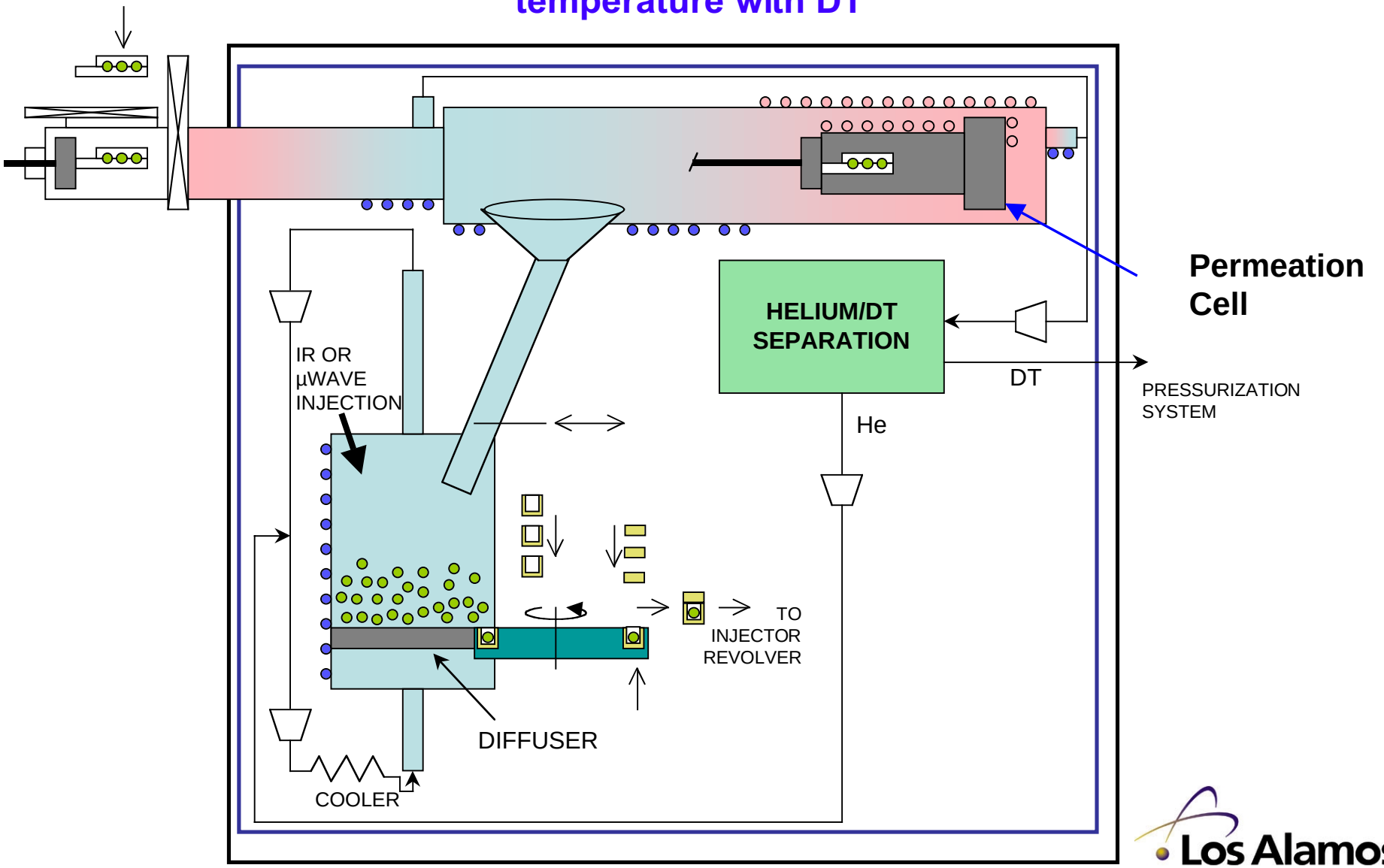

Los Alamos
NATIONAL LABORATORY

GENERAL ATOMICS
AND AFFILIATED COMPANIES

Target factory implementation

Capsules are cooled to cryogenic temperature and transferred to a fluidized bed for layering of DT

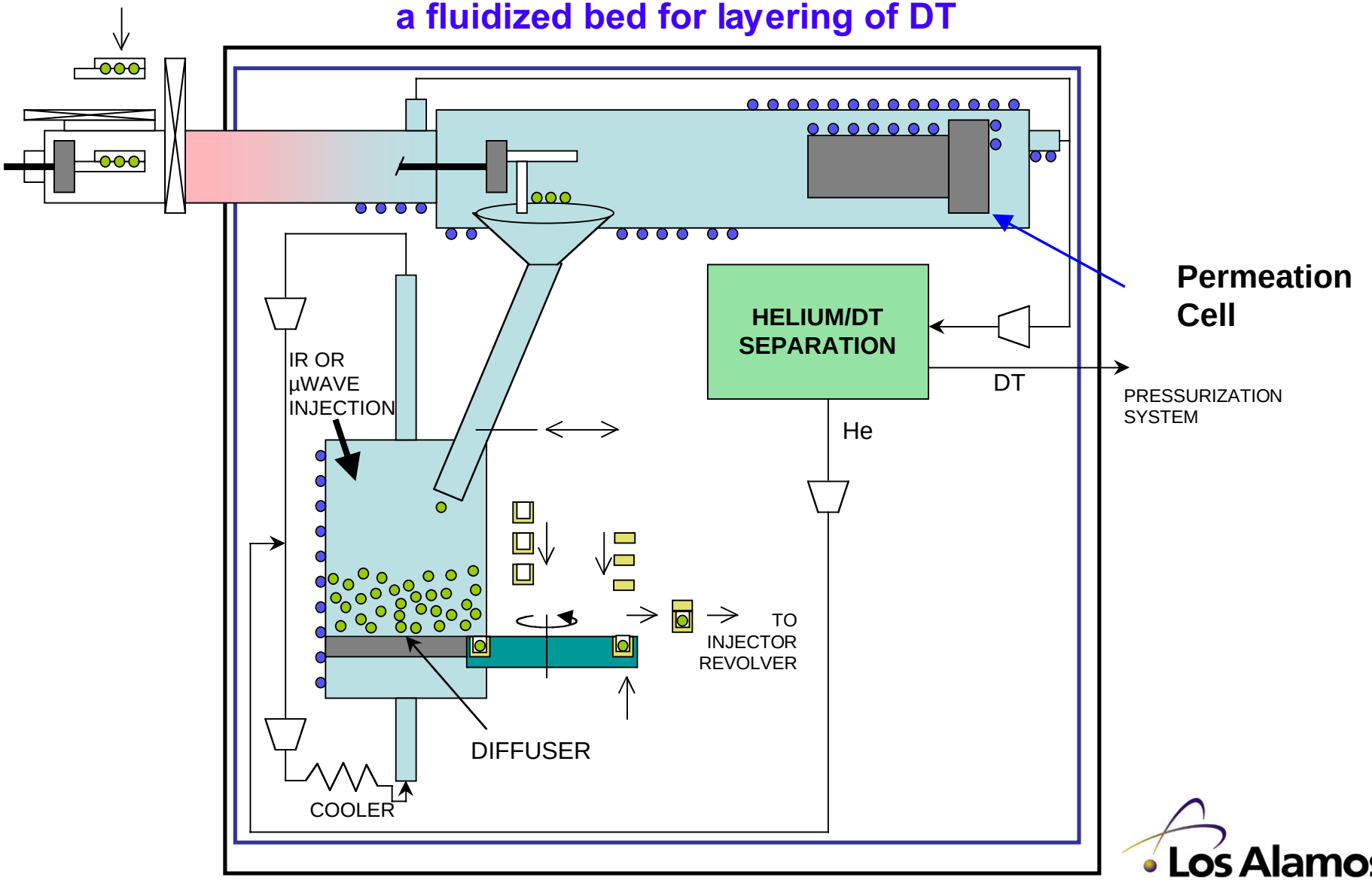

Los Alamos
NATIONAL LABORATORY

There are several possibilities for circulating the bed gas

Once through flow

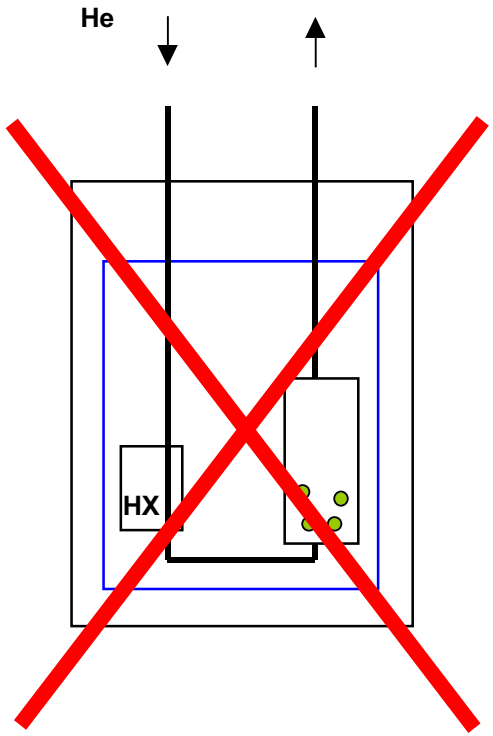

Gas bottles insufficient for long runs,
Impurity ice up of bed and windows

Room Temperature Compressor

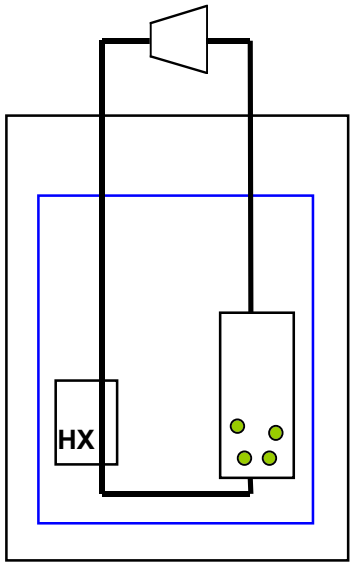

Standard technology, but
A lot of cooling required

Cryogenic Compressor

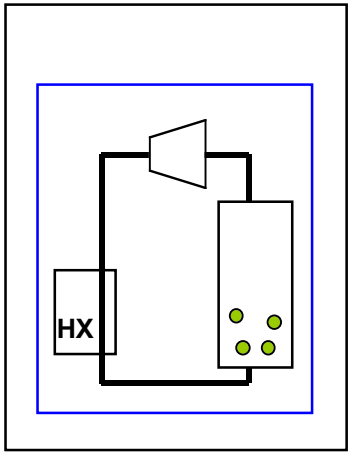

Minor cooling required,
but compressor is a
development effort

Los Alamos
NATIONAL LABORATORY

Mass flow and cooling needs can be large

BED Diameter	TARGET Diameter	Mass flow gm/sec	Cylinders of He gas/day	# of cryocoolers w/ LN2 precool	LHe/hr w/LN2 precool
34	4	1.8	103	29	145
34	1	0.9	51	14	73
10	1	.066	4	1	5

66 targets/layer

Once through

Room temperature compressor

Full size target experiment should use cryocompressor

Reduced ID bed with 1/4 scale target can operate with room temperature compressor and one cryocooler

High pressure permeation cells already designed and fabricated with 34 mm ID's
Cryocooler assumed to have 20 watt cooling power

Los Alamos NATIONAL LABORATORY

Filled targets need to be transferred into the bed

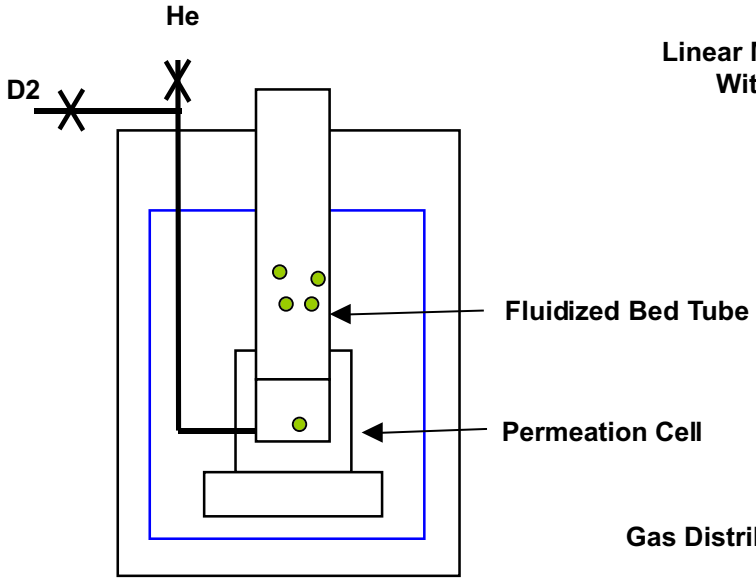

Use high pressure line to blow capsules into bed?
NO! Pressure drop in high pressure line too high (ID is 0.020")

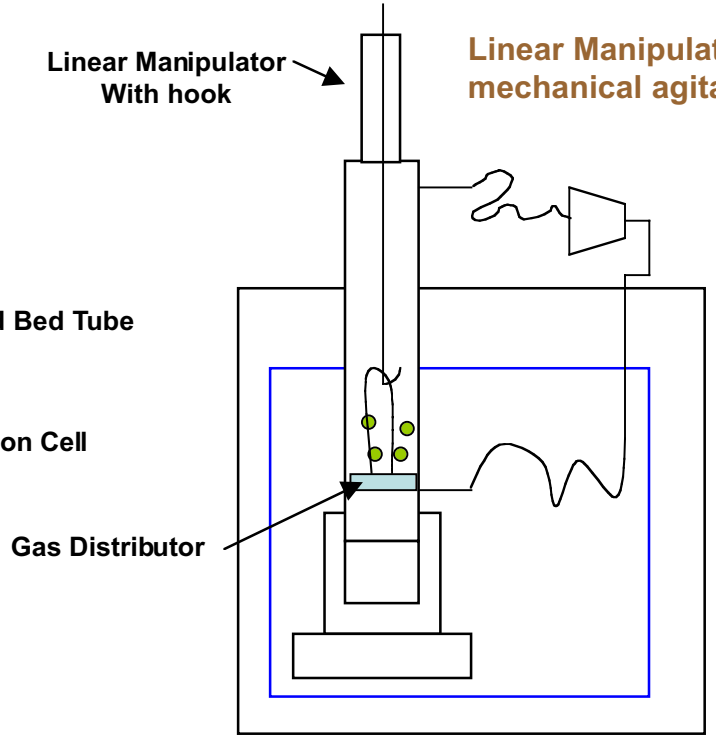

Linear Manipulator could also be used for mechanical agitation

Solution
Mechanically fish out a basket of filled targets

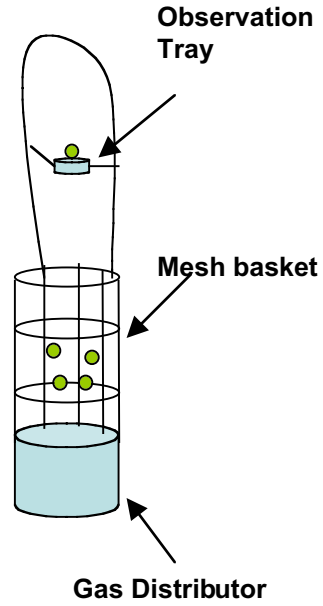

Why not use the "factory" configuration?
– We don't want to have to worry about static problems any more than we have to!

Los Alamos
NATIONAL LABORATORY

1 mm Target, Ø10 mm Bed

Compressor can likely be a rotary vane vacuum pump

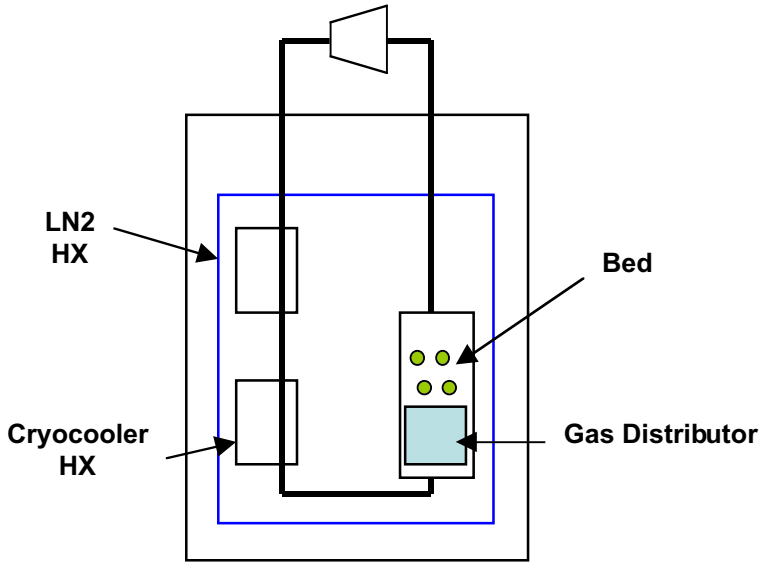

P bed = 380 torr
Mass flow = 0.066 gm/sec helium

Max. System Pressure drop < P max pump – P bed
< 760 torr – 380 torr = 380 torr

ΔP bed = 0.85 torr (11.4 cm settled height with x2 expansion)
ΔP frit = ~3 torr (want a few times bed for bed operation)
ΔP elbows = 0.01 to 0.2 torr (4 elbows)
ΔP circulation path = 0.017 to 0.2 torr (10 mm ID x 2 m long)
ΔP HX cryocooler = 72 to 150 torr (1 mm ID x 17 cm)
ΔP HX LN2 = TDB

Looks good to use vacuum pump if ΔP HX LN2 can be made as low as ΔP HX cryocooler

Los Alamos
NATIONAL LABORATORY

Permeation cell plug will be swapped with bed tube

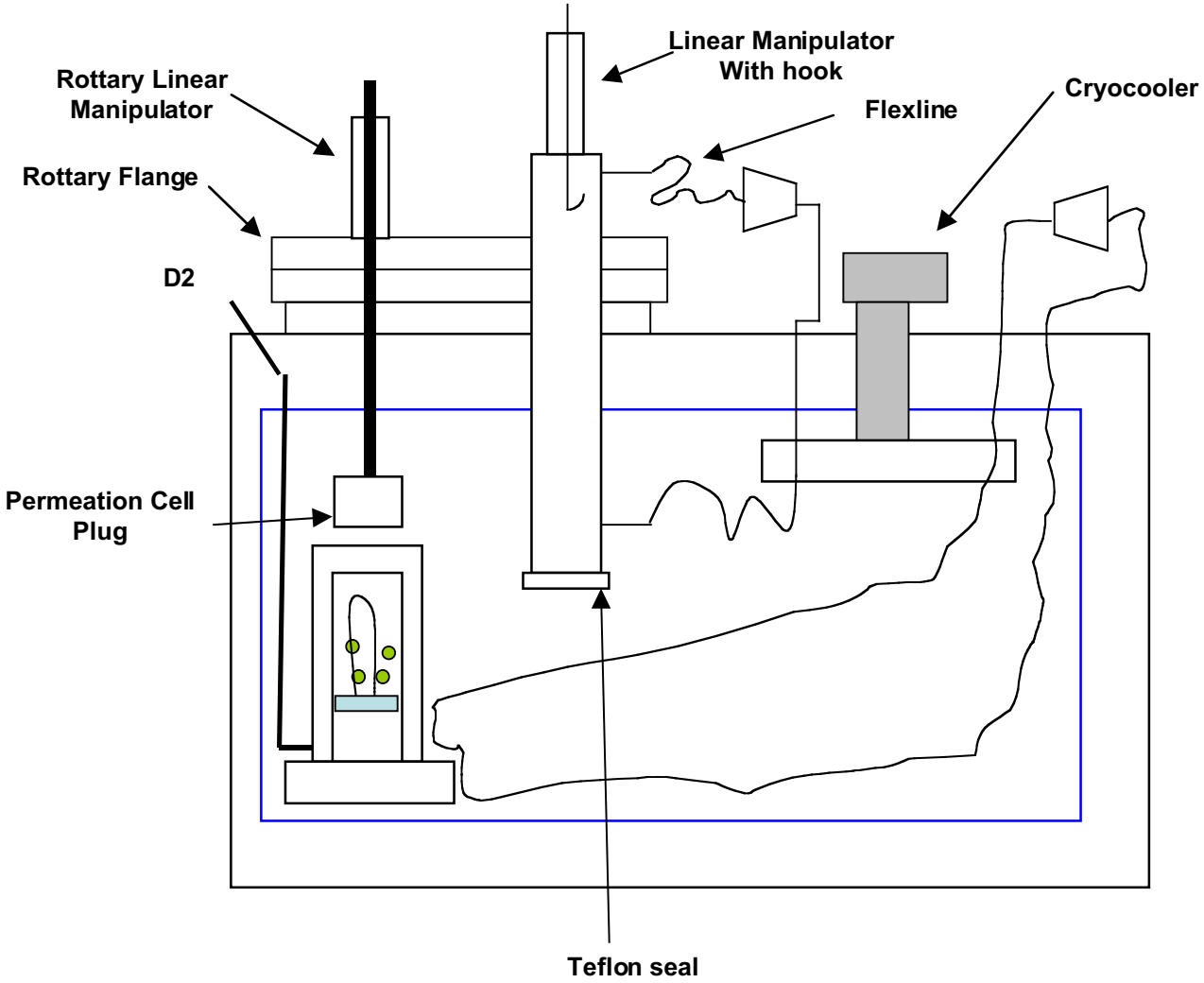

Summary and conclusions

- Demonstration of mass-production layering is a high priority for target fabrication
- A new methodology is needed for mass-production layering for IFE
  - based on demonstrated layering principles
  - methods for mechanical motion have been evaluated
- A "simple" (once through) fluidized bed at full-scale will be prohibitively expensive in operations cost
- A recirculating cryo-system will reduce operations cost - but increases the technical risk and equipment cost of the demonstrations
- A tradeoff of scale and risk will be needed
  - other ideas and concepts are certainly solicited
  - we're leaning towards an experiment using demonstrated technology at subscale - comments welcomed!